CDF/DOC/BOTTOM/CDFR/5145
Version 1
October 12, 1999

Tests of Photomultiplier Tubes for the CDF Time-of-Flight Detector

II: Tests in a Magnetic Field

Akifumi Kazama, Shigenobu Motohashi, Koji Sato†, Takashi Asakawa,
Fumihiko Ukegawa and Shinhong Kim
Institute of Physics, University of Tsukuba
†Visitor from *ICEPP, University of Tokyo*

Abstract

Two Hamamatsu R5946mod fine-mesh photomultiplier tubes have been tested for their gain and timing in the presence of a 1.44 T magnetic field using the Ushiwaka magnet at KEK. We find that the tube gain is reduced by a factor of about 500 to 1000 in the 1.44-T field. The loss in gain can be recovered by raising the operational high voltage, and the timing resolution measured with a suitable signal pulse height does not show much degradation compared with the case of no magnetic field.

1 Introduction

This is a continuation of the work presented in CDF 4980, where we tested two of the Hamamatsu R5946mod 19-stage fine-mesh photomultiplier tubes, to be used for the CDF time-of-flight (TOF) detector. The previous tests were done in the absence of any significant magnetic field. In this note we repeat the tests, although not in exactly the same ways, in a 1.44 T magnetic field using the Ushiwaka magnet, which resides in the $\pi 2$ beam line of the 12-GeV/c proton synchrotron at KEK. The tests were performed in June 1999.

The tubes we tested are the same as in CDF 4980. Hamamatsu has now assigned a new model number for this type of tubes, presumably to avoid confusion with the original 16-stage version. The new model number is R7761. The tubes used for the test have the serial numbers ZH5122 and ZH5126. They are equipped with a base assembly made by Hamamatsu. The schematic diagram of the divider circuit can be found on the web:

`http://hep-www.px.tsukuba.ac.jp/~ukegawa/tof/990415`

2 Tests

2.1 Setup

For the measurements this time we have used a different system than in the tests described in CDF 4980. In the previous test, we used a Hamamatsu precision diode laser that emits light with a 415 nm wavelength (through a frequency doubler crystal). This was a very useful device, but it belongs to our Nuclear Physics colleagues and it was not always at our disposal.

We now use a nitrogen laser, which emits ultraviolet light (337 nm). We excite a small piece of Bicron BC408 scintillator with the laser light, and the PMTs will see the scintillation light. The presence of the scintillator inevitably introduces additional time jitter because of a finite (about 2.5 ns) decay time of the BC408 scintillating material. On the other hand, one can regard this method to be more realistic, because in the end we will be detecting photons produced in by the BC408 scintillator.

The setup of the tests is shown schematically in Figure 1. Initially we tried to operate the nitrogen laser with an external trigger pulse (TTL), with the hope of using the external pulse as a reference for timing measurements. It has turned out that the timing jitter of light emission with respect to this external trigger is not as accurate (typically of order 100 ns) as we would like ($\ll 100$ ps). Therefore, we needed to obtain our own reference of timing measurements. For this purpose, we split the laser light into two beams using a half mirror and detect one of them using a PMT, whose signal is used as a trigger and as a reference for timing measurements. In that case there is no reason to operate the laser with an external pulse, so we operate it in an internal mode. The repetition rate is set to be about 1 Hz.

We direct the split light through a fiber optic cable to a Hamamatsu H1161 PMT, where no scintillator is placed between the light and the photocathode. There are two identical anode signals from H1161 PMTs. One of them is discriminated and is used to start the CAEN C414 TDC (25 ps per count). The other anode signal is fed into the Kaizu ADC for monitoring purposes. The photocathode of H1161 PMTs is well sensitive to ultraviolet light, and by injecting a large enough amount of light we are able to obtain a timing signal with a small jitter. The jitter is estimated by using two beams of split light, directed to two H1161 PMTs, by measuring the spread of the difference in the arrival times (discriminated signals) from the two PMTs. The rms spread is measured to be about 45 ps, meaning that the contribution from each tube is about 30 ps. This is good enough for the present test purposes.

When testing the fine-mesh tubes, the second beam of the split light is directed through a fiber optic cable to a small (1 cm by 1 cm by 3 cm) piece of Bicron BC408 scintillator placed in front of the face of the fine-mesh PMT that resides in the magnet. There is an air gap between the output of the fiber optic and the PMT cathode.

The analog signal from the fine-mesh PMT goes through the LeCroy 428F linear fanout and is split into two. One of them is discriminated to provide the stop signal for timing measurements and an ADC gate, and the other is fed to the ADC for pulse height measurements.

2.2 Measurements without magnetic fields

First we have tested the tubes without applying any current to the Ushiwaka magnet. The results are given in Figures 2 and 3 for the two tubes, ZH5122 and ZH5126, respectively. The tubes are operated with high voltages of +1200 V and +1250 V. The timing resolutions are 4.03 and 3.34 TDC counts, or 101 ps and 83 ps, respectively.

The resolution here is not as good as that reported in CDF 4980 using the Hamamatsu diode laser. But has been is expected because there is contribution from the finite scintillator decay time (2.5 ns), which is absent when we used the diode laser and injected light with a 415 nm wavelength directly to the PMTs.

Also, a careful reader might notice that we now see slightly larger pulses with ZH5126 than with ZH5122. This was not the case in the previous test, e.g. Fig. 9 of CDF 4980. In the previous test, we used two separate HV supplies for the two tubes. Between now and then, we found a HV supply used for ZH5126 had been bad, and we suspect that the HV value at the tube ZH5126 really had been lower than indicated at the settings. Therefore, one should not believe anything in CDF 4980 that is related to pulse heights and gains of ZH5126.

2.3 Pulse height measurements in magnetic fields

Now we energize the magnet and apply the magnetic field to the PMTs. We gradually increased the magnetic field strength, and eventually we have set the controller voltage to 3.6 V, which produces a magnetic field of about 1.44 T. The relation may be found on the web:

`http://hep-www.px.tsukuba.ac.jp/~ukegawa/tof/ushiwaka.jpg`

The observed mean pulse height as a function of the magnetic field is shown as filled circles in Figures 4 and 5 for tubes ZH5122 and ZH5126. The gain at the full field is smaller than that at zero field by a factor of somewhere between 500 to 1000. This confirms the nominal reduction observed by Hamamatsu for those tubes, shown at:

`http://hep-www.px.tsukuba.ac.jp/~ukegawa/tof/9903/`

Then we raised the high voltage applied to the tubes and measure pulse heights, while keeping the magnetic field at 1.44 T. They are shown as open circles in the figures. We can see that the gain is recovered with an increasing high voltage value, and eventually comes (almost) to the original value at 2500 and 2700 V, respectively.

Figures 6 and 7 show the mean pulse height as a function of the high voltage value applied to the PMTs.

2.4 Timing measurements in magnetic fields

We examine the data taken with the full magnetic field and the highest voltage settings for timing performance. The pulse height and arrival time distributions are shown in Figures 8 and 9. The timing resolutions are 4.73 and 3.63 counts, or 118 ps and 91 ps, respectively, for ZH5122 and ZH5126. These numbers are about 10 to 15% worse than the resolutions at $B = 0$ T, namely 101 ps and 83 ps seen at similar pulse heights.

2.5 Estimating gains

Figures 10 and 11 show the mean pulse height as a function of the high voltage value applied to the PMTs. Here we have added data points taken at $B = 0$ T at several high voltage settings.

Each of the two sets of pulse height measurements, taken at $B = 0$ T and $B = 1.44$ T, shows a linear dependence on the high voltage when plotted on log-log scales. Thus, we try to describe the high voltage dependence of the pulse height in the following form:

$$Q(V) = \beta(V/V_0)^\alpha,$$

where $Q(V)$ is the pulse height observed at a voltage V, and V_0 is an arbitrary reference voltage (we choose to be 1000 V in this note), α and β are free parameters and are determined them from a fit. The parameter values obtained from the fit are given in Table 1. We see that there is little difference in the parameter α between the two tubes and with and without the magnetic field. This parameter, obviously, governs the high voltage dependence.

We then calculate the expected charge at $V = 2000$ V for both $B = 0$ and 1.44 T, using the formula above and the parameters α and β determined from the fit. It is also shown in Table 1, along with a measurement at $B = 1.44$ T.

We can estimate the gain of the tubes at 2000 V and $B = 1.44$ T, by using a gain measurement done by Hamamatsu at the same voltage and with the absence of a magnetic field, once we assume that the quantum efficiency, defined so that it includes the photo-electron correction efficiency, is constant regardless of the high voltage setting and of the presence/absence of a magnetic field. To be specific, we use the formula

$$G(1.44\ \mathrm{T}, 2000\ \mathrm{V}) = G(0\ \mathrm{T}, 2000\ \mathrm{V})\ \frac{Q(1.44\ \mathrm{T}, 2000\ \mathrm{V})}{Q(0\ \mathrm{T}, 2000\ \mathrm{V})},$$

where G are gains, and $G(0\ \mathrm{T}, 2000\ \mathrm{V})$ comes from Hamamatsu, and Q are calculated from the fit parameters.

One can simply extend this formula to an arbitrary value of high voltage setting at $B = 1.44$ T. The gains estimated this way are listed in Table 2. The gains in the 1.44 T

Tube	B (T)	α	β	Q (2000 V) (measured) (ADC count)	Q (2000 V) (calculated) (ADC count)
ZH5122	0	8.24 ± 0.04	63.8 ± 0.4	–	19301 ± 581
	1.44	8.04 ± 0.01	0.145 ± 0.001	37.8 ± 0.4	38.1 ± 0.2
ZH5126	0	8.55 ± 0.03	93.1 ± 0.5	–	34891 ± 740
	1.44	7.91 ± 0.03	0.162 ± 0.004	37.9 ± 0.6	39.2 ± 0.8

Table 1: High voltage dependence of the observed charge, and measured and calculated charge at a high voltage of 2000 V with and without magnetic fields.

Tube	B (T)	Gain (2000 V) ($\times 10^6$)	Gain (2500 V) ($\times 10^5$)	HV (1×10^5) (V)	HV (3×10^5) (V)
ZH5122	0	155.1			
	1.44	0.306 ± 0.009	18.4 ± 0.6	1740 ± 7	1995 ± 8
ZH5126	0	65.3			
	1.44	0.073 ± 0.002	4.28 ± 0.14	2080 ± 8	2390 ± 8

Table 2: Gains estimated for $B = 1.44$ T and high voltages of 2000 V and 2500 V, using the measured charge and its high voltage dependence and the gain measured by Hamamatsu at 2000 V and $B = 0$ T. Also shown are the high voltage values necessary to obtain the gains of 1.0×10^5 and 3.0×10^5 at $B = 1.44$ T.

field at a high voltage of 2500 V are several times 10^5 for those tubes. At present the draft specifications of the tubes require the minimum tube gain of 3.0×10^5 at $B = 1.44$ T and at a high voltage of less than 2500 V.

Conversely, one can use the formula above and solve for a high voltage value that gives a certain gain in the magnetic field. We also list in Table 2 the voltage values that give gains of 1.0×10^5 and 3.0×10^5. These numbers are of some practical interest, because we could have some ideas about the maximum high voltage that the power supply has to provide for the real detector in B0.

The two tubes we tested satisfy the gain requirement above. However, more recent indications from Hamamatsu are that these tubes in the earlier production batch are on a high side of the gain distributions. A typical gain at $B = 0$ T and 2000 V is now more like 3×10^7 rather than 7×10^7 as previously indicated in CDF 4980. Therefore, we might want to revise the minimum gain requirement slightly, e.g. to 1.0×10^5 in the magnetic field. Tests done by Matthew Jones and his colleagues at Penn indicate that we would still be able to perform precise timing measurements with that gain. Also, the maximum anode current rating of 10 μA will likely prevent us from operating those tubes with a gain much higher than 1.0×10^5.

3 Conclusions

We have tested two of the Hamamatsu H7761 19-stage fine-mesh PMTs, to be used for the CDF TOF detector, at the presence of a 1.44 T magnetic field using the Ushiwaka magnet located in the $\pi 2$ beam line of the 12-GeV proton synchrotron at KEK.

We find that the pulse height is reduced by a factor of 500 to 1000 in the 1.44 T axial magnetic field. However, timing resolution does not degrade much (only about 10%), after high voltages applied to the tubes are raised and pulse height is restored to a similar level.

Acknowledgment

We would like to thank Professors Takahiro Sato and Yoshio Yoshimura of KEK for their help and arrangements in using the Ushiwaka magnet at KEK.

A PMT inventory

The following tables show the inventory of the tubes as of September 30, 1999.

R7761 DC Sensitivity

Serial Number		Cathode luminous sensitivity (μA/lm)	Anode luminous sensitivity (A/lm)	Anode dark current (nA)	Cathode blue sensitivity (μA/lm-bl)	Gain (10^6)
ZH5121	(Penn)	77.0	7260	150	9.71	94.3
ZH5122*	(Tsukuba)	51.9	8050	16.00	8.4	155.1
ZH5123	(Penn)	76.5	4610	7.20	9.83	60.3
ZH5126*	(Tsukuba)	81.5	5320	9.30	10.1	65.3
ZH5129	(Tsu $\rightarrow$ P)	75.4	11400	11.00	9.9	151.2
ZH5132	(Tsu $\rightarrow$ P)	82.7	2080	1.10	10.4	25.2
ZH5134†	(Tsu $\rightarrow$ P)	58.3	1730	1.0	9.2	29.7
ZH5136	(Tsukuba)	76.5	3680	2.50	10.2	48.1
ZH5137		87.9	2040	1.7	10.4	23.2
ZH5138†	(Tsu $\rightarrow$ P)					

Table 3: Cathode and anode luminous sensitivity of R7761 tubes. Reproduced from data sheet provided by Hamamatsu. Measurements of anode sensitivity and dark current are made at a high voltage of 2000 V. Tubes with (*) are equipped with base assembly made by Hamamatsu. Tubes with (†) are provided by Hamamatsu as mechanical samples, but they might actually work.

R7761 Tubes (from the order of 44 tubes, made June 1999)

Serial Number		Cathode luminous sensitivity (μA/lm)	Anode luminous sensitivity (A/lm)	Anode dark current (nA)	Cathode blue sensitivity (μA/lm-bl)	Gain (10^6)	Delivery Date
ZH5124*		81.8	3700.	0.65	10.10	45.2	990701
ZH5125*		74.6	2710.	77.00	9.96	36.3	990701
ZH5127		72.6	6820.	34.00	9.83	93.9	990701
ZH5128	(Tsu $\rightarrow$ P)	57.4	4380.	2.40	9.01	76.3	990701
ZH5130	(Tsu $\rightarrow$ P)	79.5	7230.	9.40	9.96	90.9	990701
ZH5131	(Tsu $\rightarrow$ P)	65.2	3230.	2.20	9.24	49.5	990701
ZH5133	(Tsu $\rightarrow$ P)	64.0	2200.	9.60	9.35	34.4	990701
ZH5135	(Tsu $\rightarrow$ P)	63.4	7540.	7.40	9.91	118.9	990701
ZH5139	(Tsu $\rightarrow$ P)	90.8	1870.	0.55	10.40	20.6	990701
DA0001		87.3	2360.	13.	11.20	27.0	990804
DA0011		89.9	4100.	4.5	10.80	45.6	990804
DA0036		93.8	3310.	2.8	10.70	35.3	990804
DA0037		104.	2740.	5.1	11.20	26.3	990804
DA0038		93.2	3280.	15.0	10.70	35.2	990804
DA0043		99.5	3160.	5.7	11.30	31.8	990804

(continued on the next page)

Serial Number	Cathode luminous sensitivity (μA/lm)	Anode luminous sensitivity (A/lm)	Anode dark current (nA)	Cathode blue sensitivity (μA/lm-bl)	Gain (10^6)	Delivery Date
DA0004	60.4	813.	0.38	9.16	13.5	990901
DA0008	92.6	1260.	5.40	10.20	13.6	990901
DA0013	77.3	1930.	11.0	9.52	25.0	990901
DA0014	90.4	1360.	2.2	10.8	15.0	990901
DA0016	83.6	1590.	4.30	10.1	19.0	990901
DA0017	87.4	1060.	3.9	10.3	12.1	990901
DA0018	80.4	1610.	1.3	10.7	20.0	990901
DA0019	61.6	1210.	1.1	9.5	19.6	990901
DA0020	79.0	967.	4.6	9.87	12.2	990901
DA0012	84.7	1770.	4.5	9.96	20.9	990906
DA0021	80.5	2610.	14.0	10.10	32.4	990906
DA0023	98.5	3120.	7.3	10.9	31.7	990906
DA0024	74.2	2200.	1.10	10.30	29.7	990906
DA0025	84.3	3210.	18.0	9.88	38.1	990906
DA0026	87.5	8090.	9.4	10.3	92.5	990906
DA0028	93.9	2300.	24.	10.4	24.5	990906
DA0029	87.4	1610.	14.	10.1	18.4	990906
DA0033	92.6	1230.	6.6	10.7	13.3	990906
DA0035	96.7	3550.	3.5	11.0	36.7	990906
DA0040	73.1	2370.	2.1	10.10	32.4	990906
DA0047	83.0	3580.	110.	9.81	43.1	990906
DA0048	67.5	5790.	130.	8.74	85.8	990906
DA0050	62.8	2340.	2.60	9.59	37.3	990906
DA0051	88.3	1160.	3.0	10.6	13.1	990906
DA0060	86.4	1160.	3.0	10.6	13.4	990906
DA0062	86.4	2120.	3.0	10.6	25.3	990906
DA0073	58.4	3640.	2.2	9.33	62.3	990906
DA0079	77.0	2200.	18.0	9.65	28.6	990906
DA0083	104.	1090.	3.0	11.40	10.5	990906

Table 4: Cathode and anode luminous sensitivity of R7761 tubes. Reproduced from data sheet provided by Hamamatsu. Measurements of anode sensitivity and dark current are made at a high voltage of 2000 V. Tubes with (*) are equipped with base assembly made by Hamamatsu.

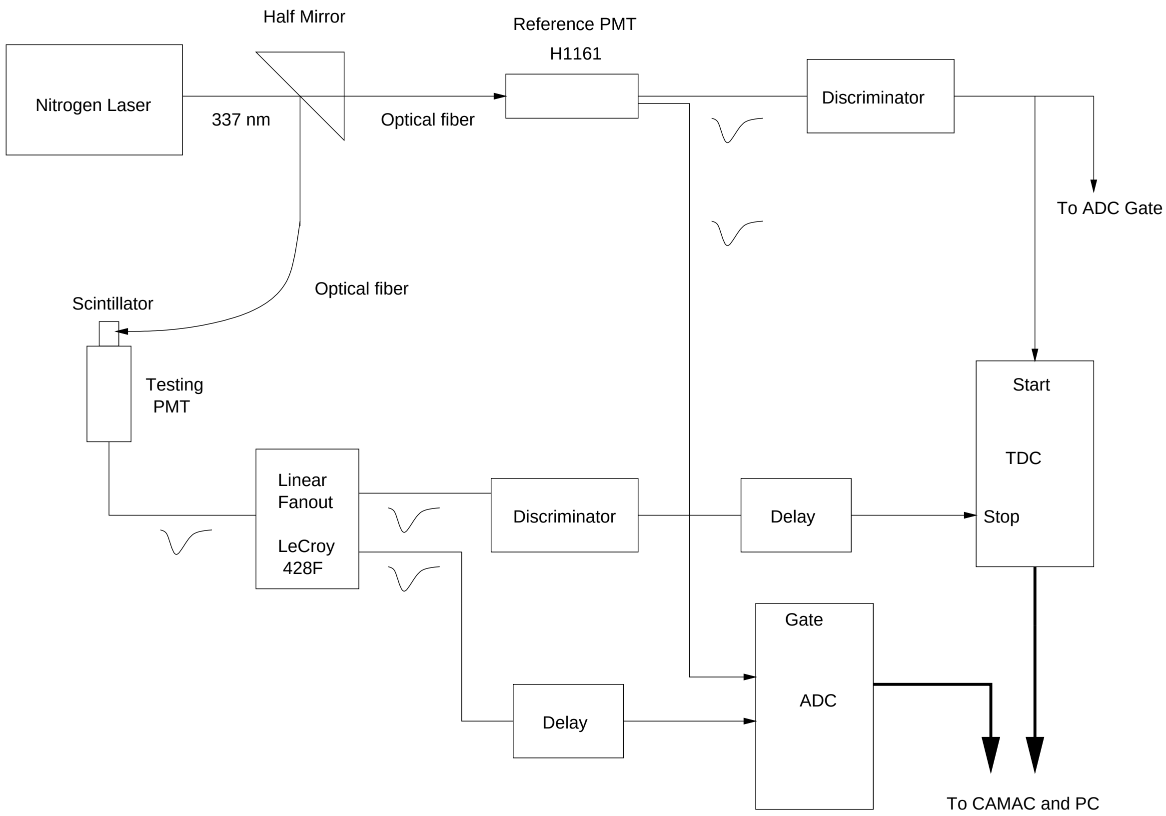

Figure 1: Setup used for the measurement of the PMT timing resolution using a pico-second laser.

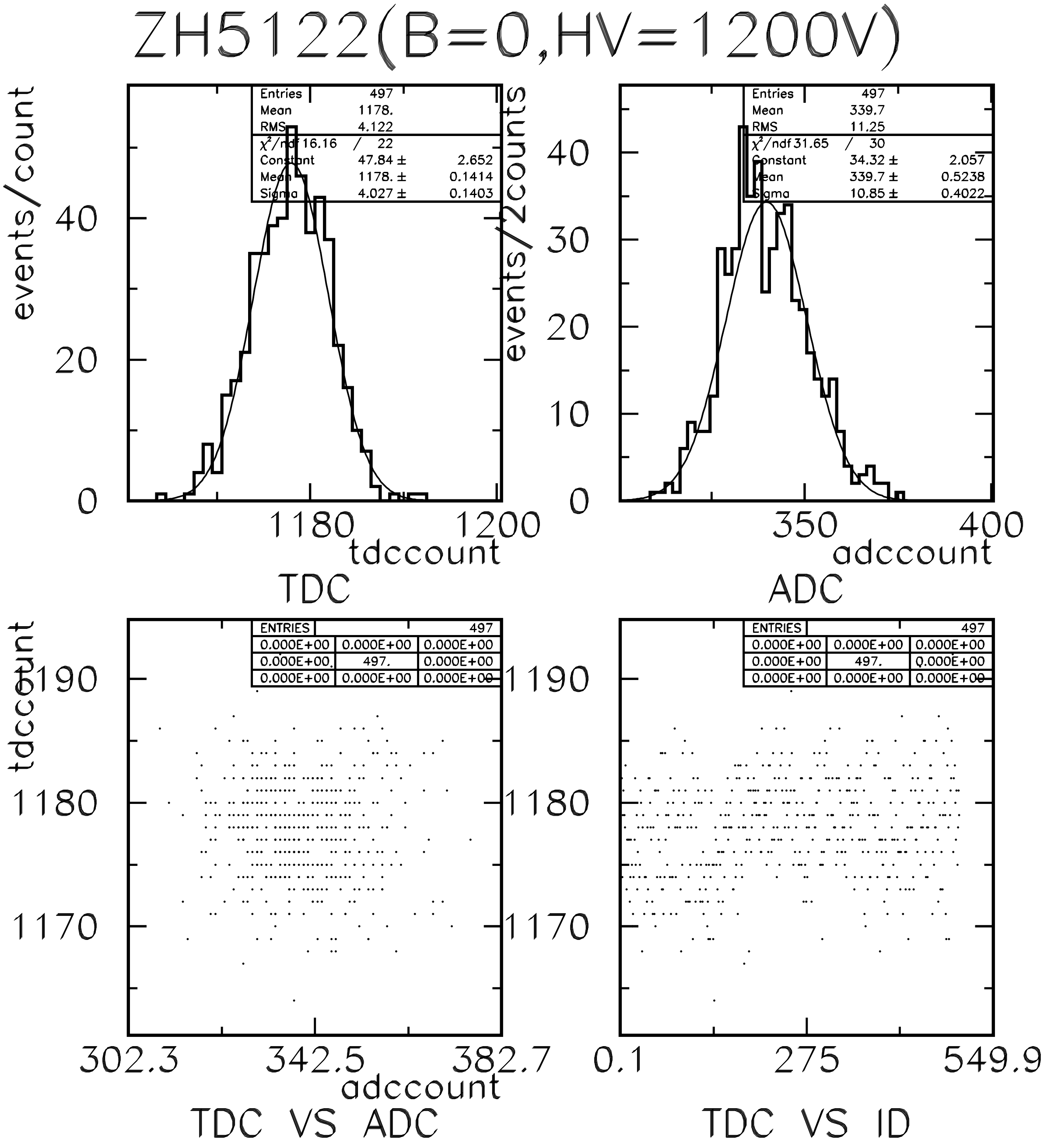

Figure 2: TDC arrival time and ADC pulse height distributions and their correlation for scintillation light measured with the tube ZH5122. The high voltage is set to 1200 V, and the discriminator threshold is set to 30 mV. There is no magnetic field applied.

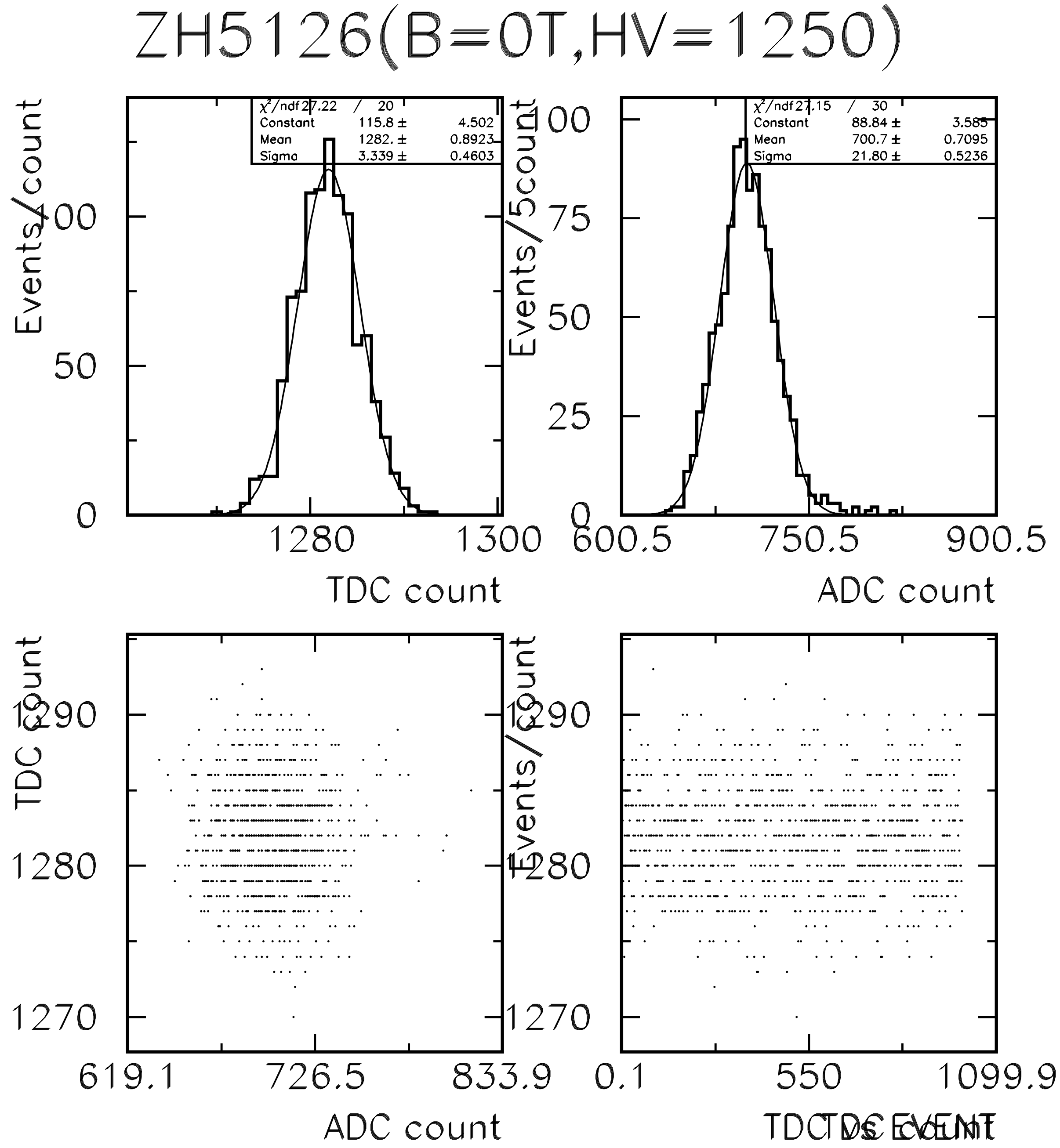

Figure 3: TDC arrival time and ADC pulse height distributions and their correlation for scintillation light measured with the tube ZH5126. The high voltage is set to 1250 V, and the discriminator threshold is set to 30 mV. There is no magnetic field applied.

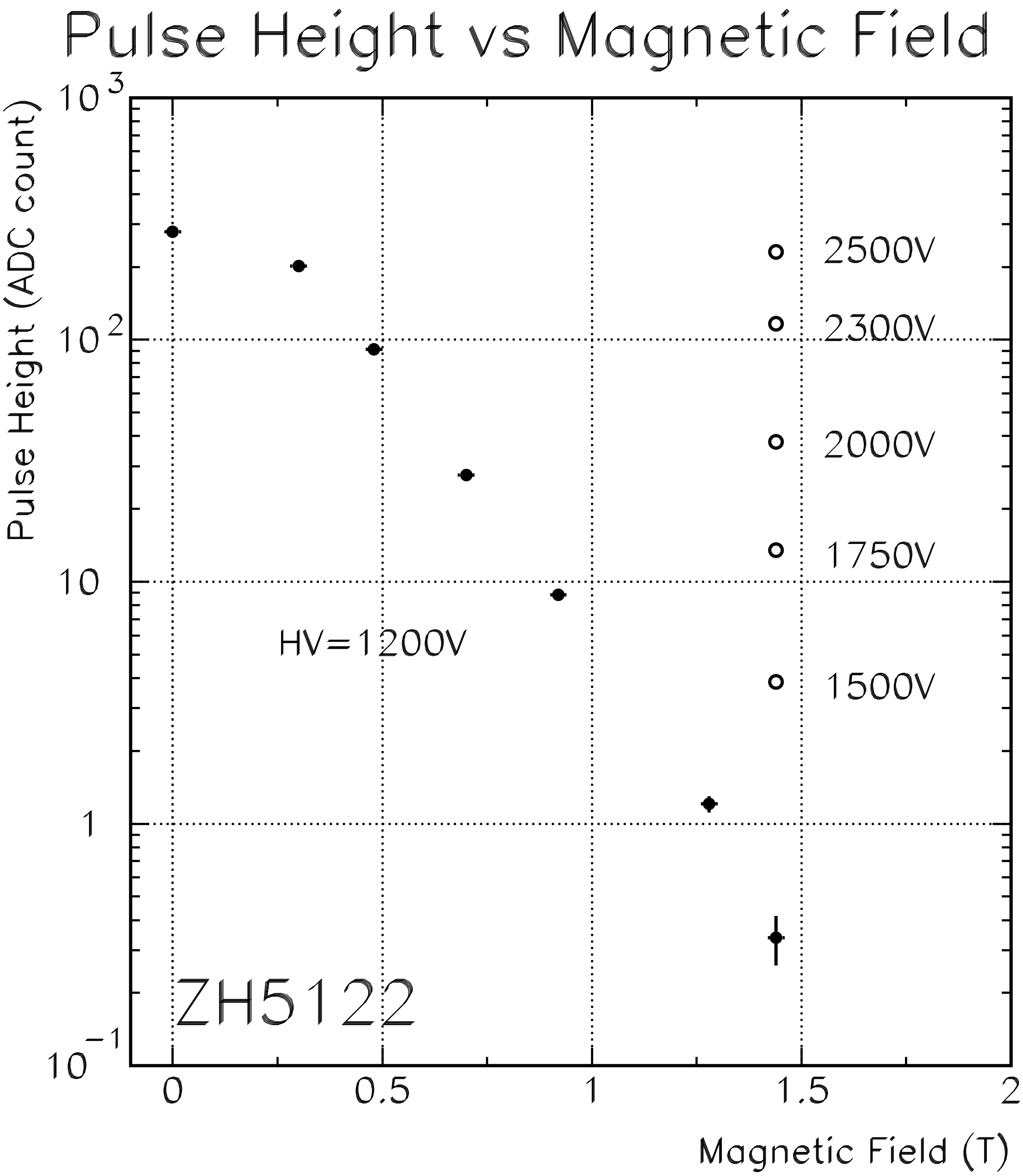

Figure 4: Mean ADC pulse height measured with the tube ZH5122 as a function of the magnetic field (filled circles) at a high voltage of 1200 V. Open circles shows mean pulse height when the high voltage is changed at $B = 1.44$ T.

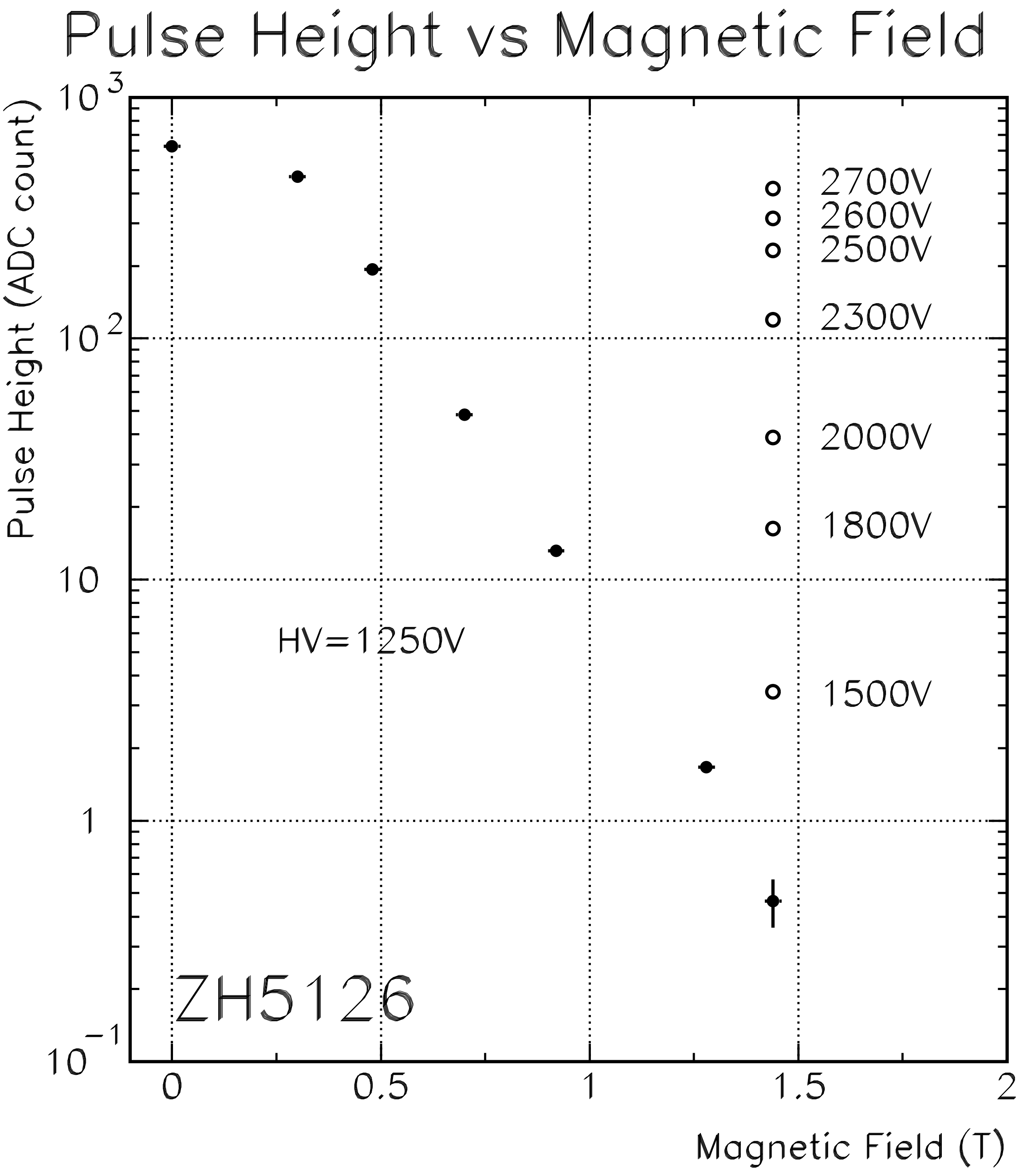

Figure 5: Mean ADC pulse height measured with the tube ZH5126 as a function of the magnetic field (filled circles) at a high voltage of 1250 V. Open circles shows mean pulse height when the high voltage is changed at $B = 1.44$ T.

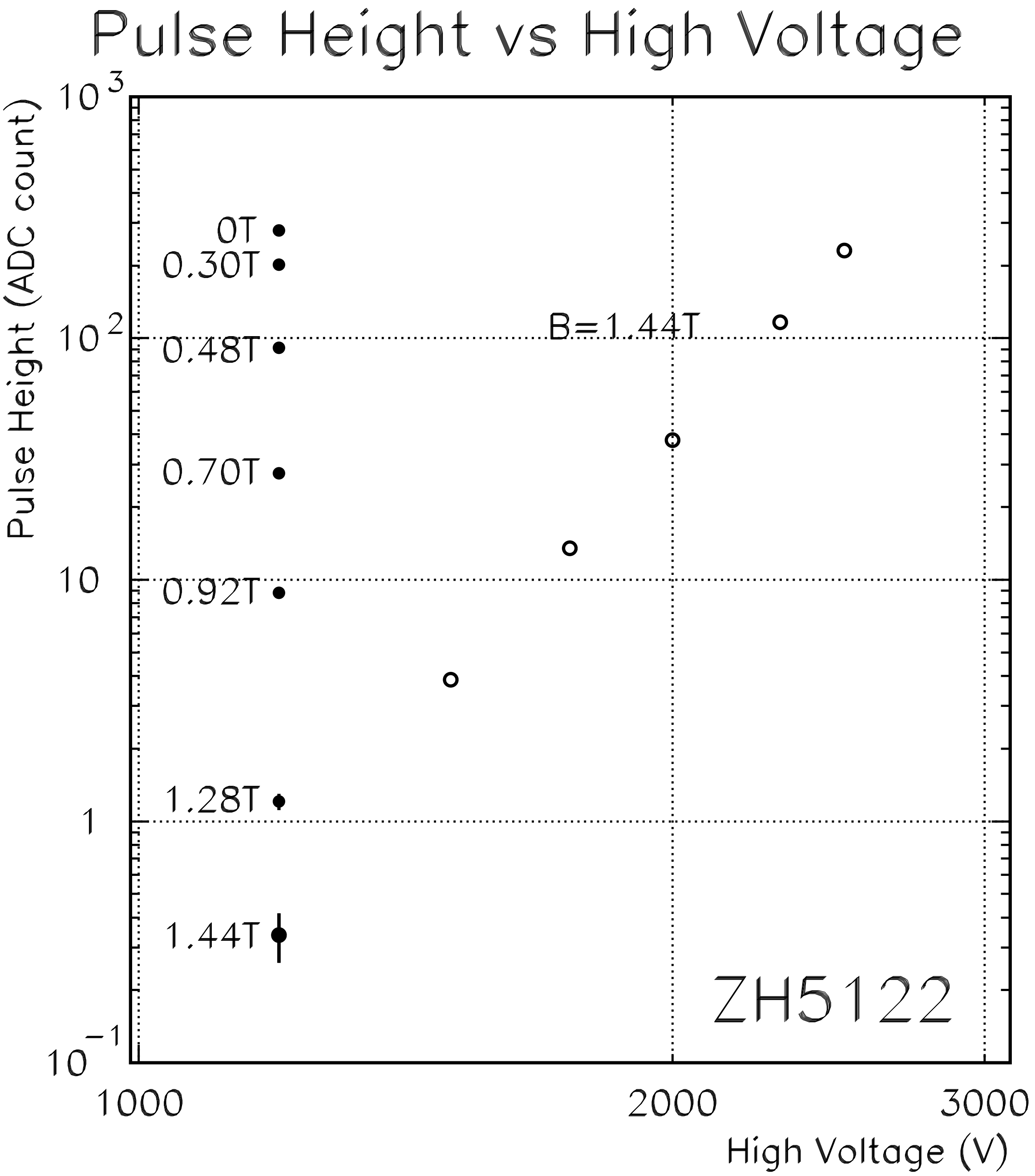

Figure 6: Mean ADC pulse height measured with the tube ZH5122 as a function of the applied high voltage value (open circles) in a magnetic field of 1.44 T. Filled circles shows mean pulse height when the magnetic field is changed while keeping the high voltage at 1200 V.

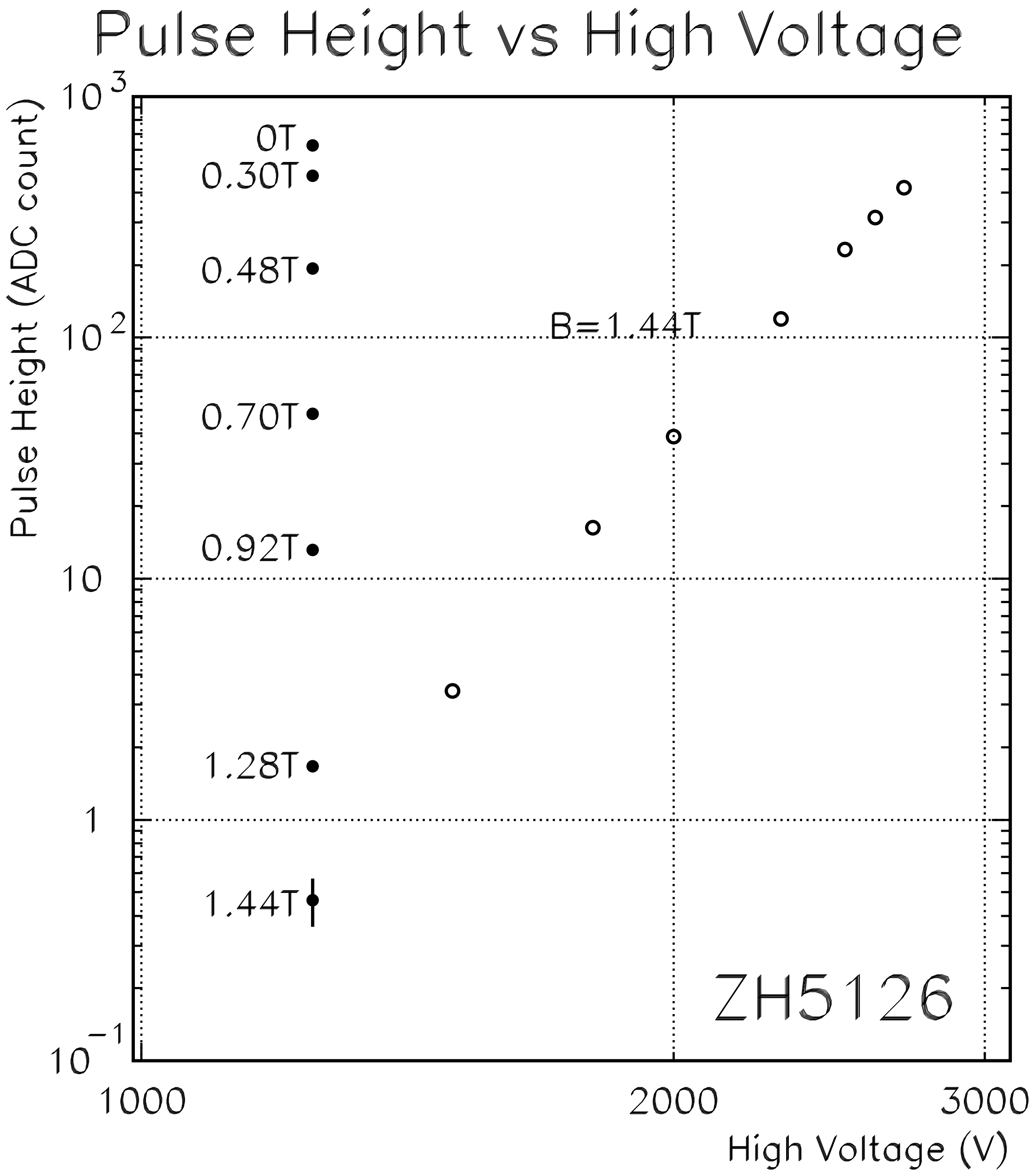

Figure 7: Mean ADC pulse height measured with the tube ZH5126 as a function of the applied high voltage value (open circles) in a magnetic field of 1.44 T. Filled circles shows mean pulse height when the magnetic field is changed while keeping the high voltage at 1250 V.

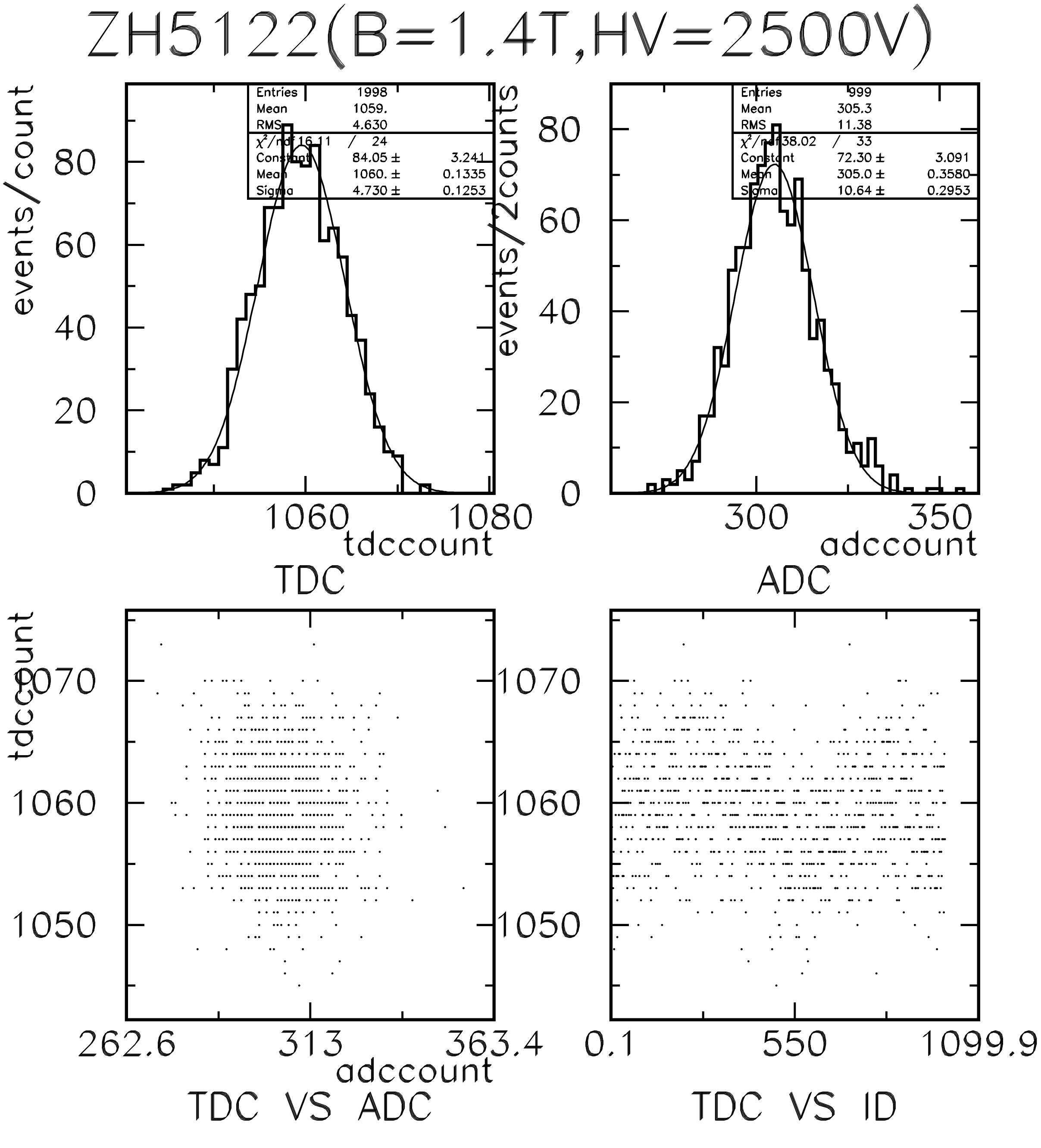

Figure 8: TDC arrival time and ADC pulse height distributions and their correlation for scintillation light measured with the tube ZH5122 inside a 1.44 T magnetic field. The high voltage is set to 2500 V, and the discriminator threshold is set to 30 mV.

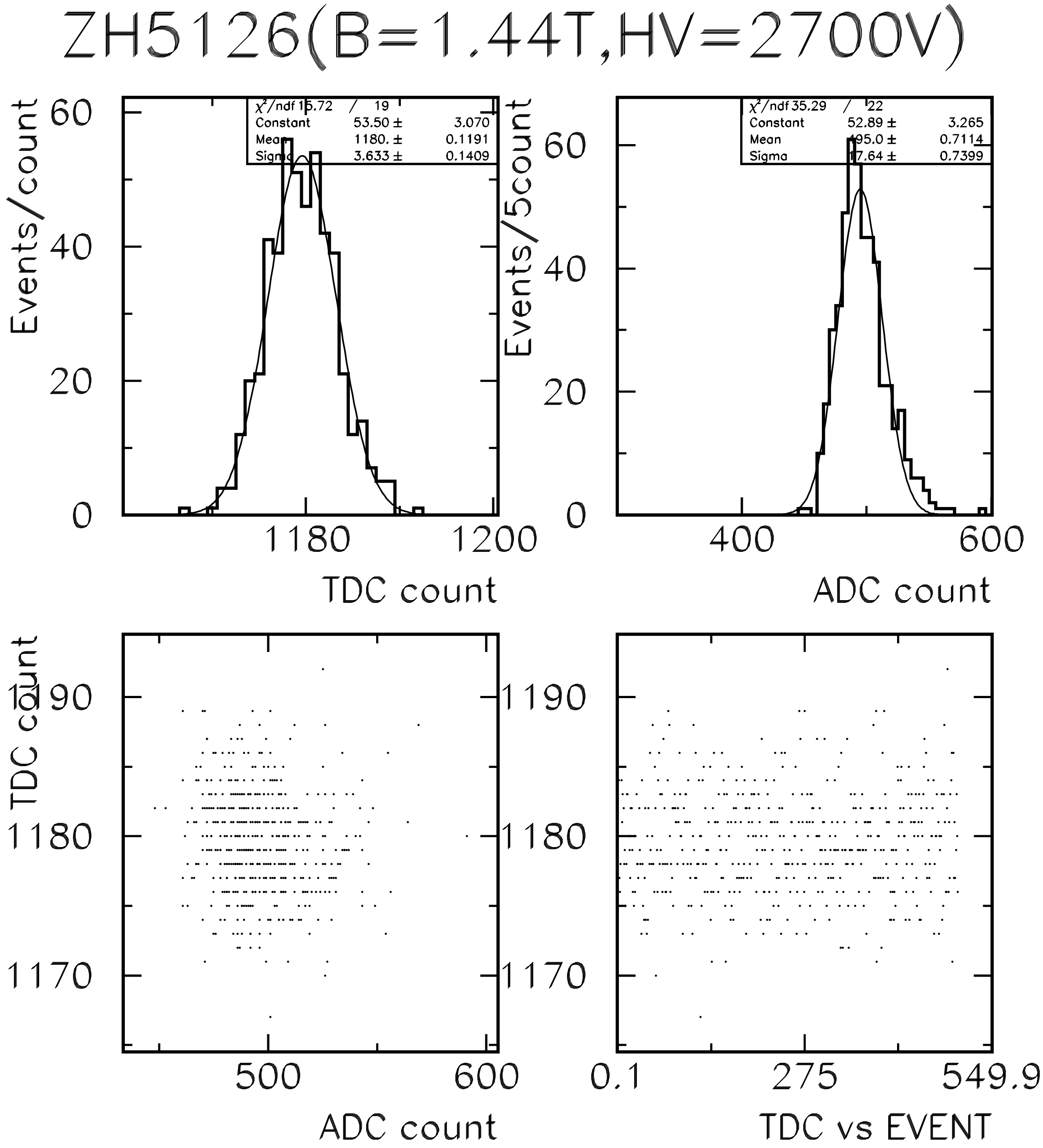

Figure 9: TDC arrival time and ADC pulse height distributions and their correlation for scintillation light measured with the tube ZH5126 inside a 1.44 T magnetic field. The high voltage is set to 2700 V, and the discriminator threshold is set to 30 mV.

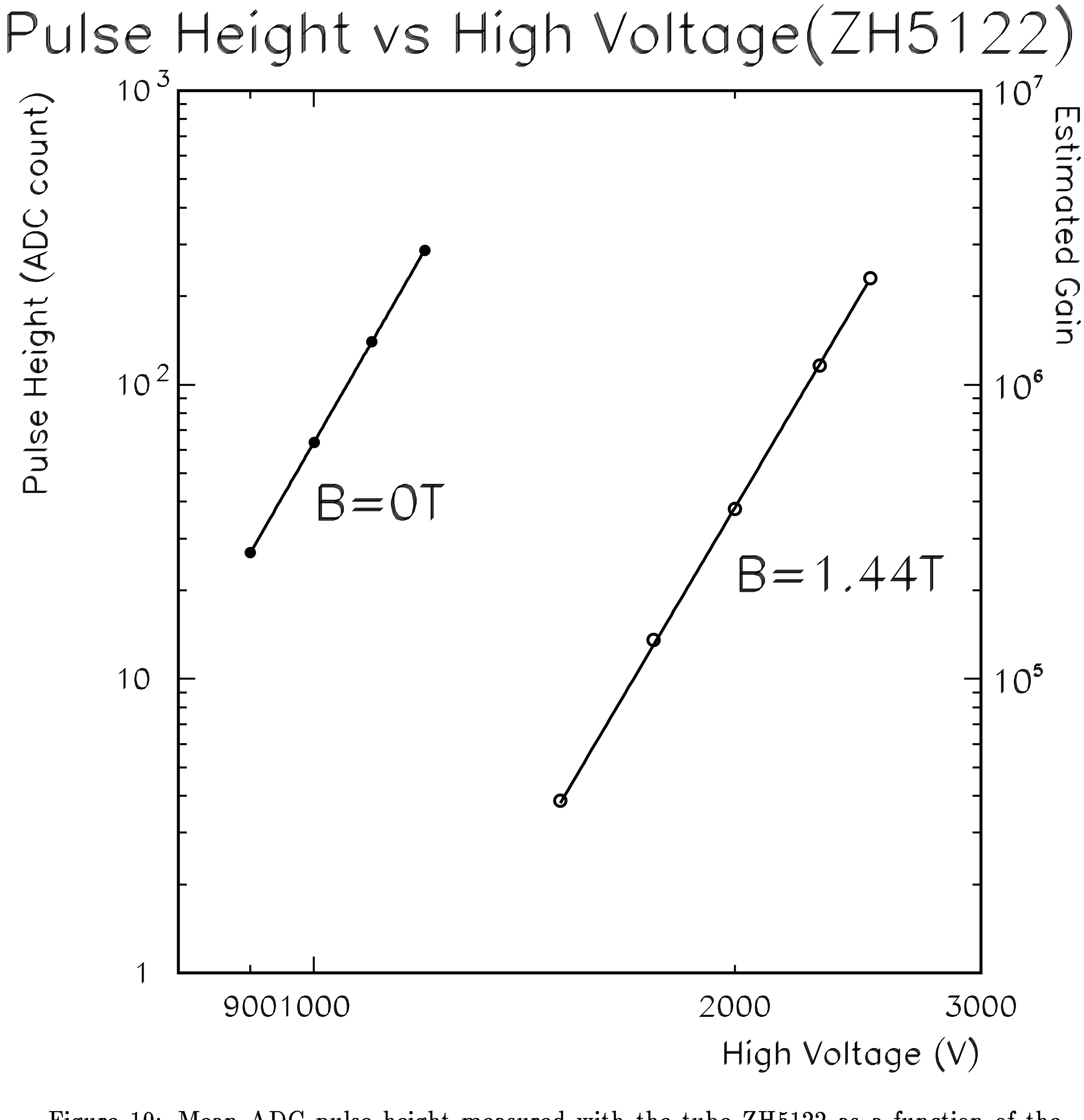

Figure 10: Mean ADC pulse height measured with the tube ZH5122 as a function of the applied high voltage value in magnetic fields of 1.44 T (open circles) and 0 T (filled circles).

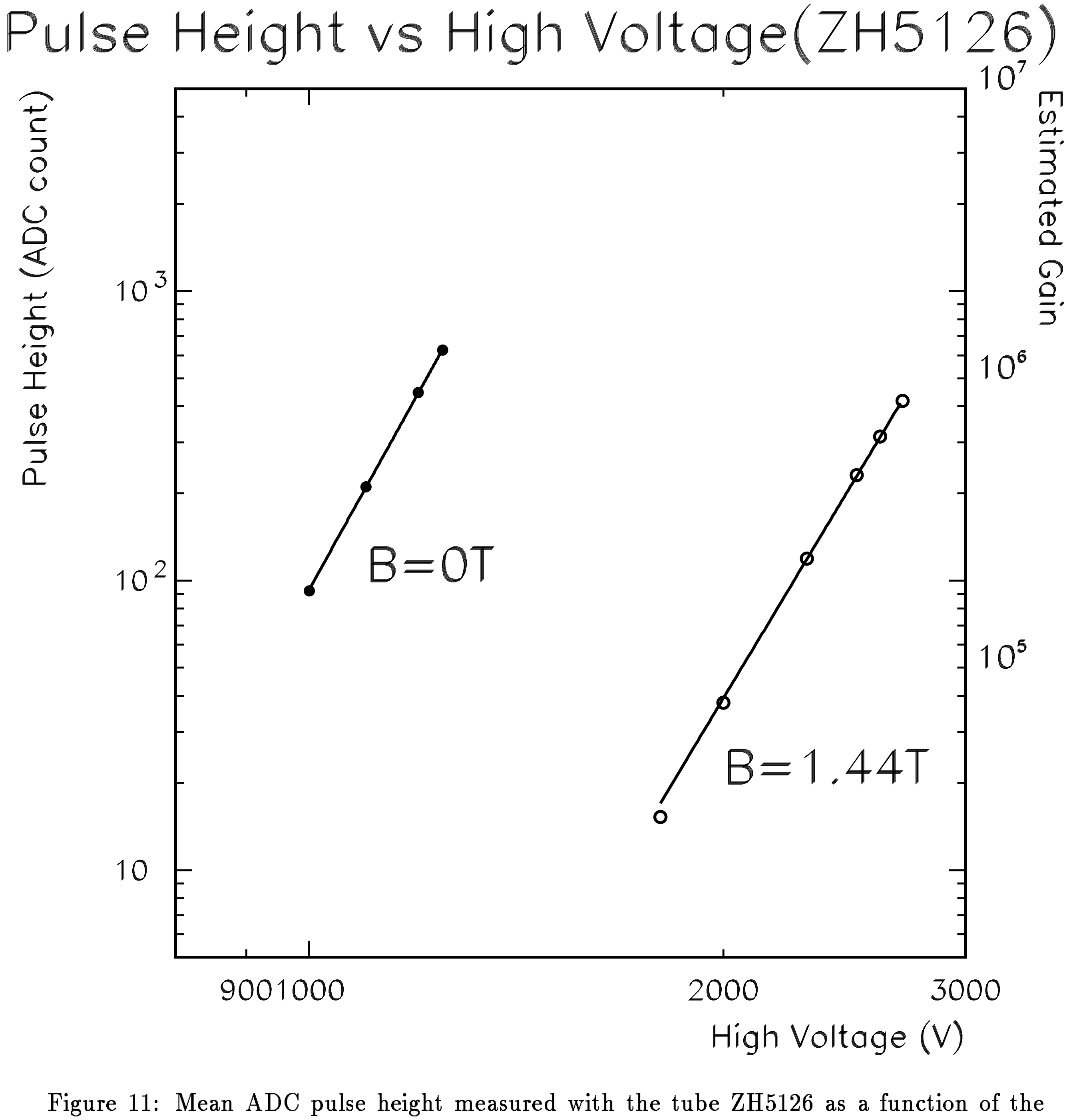

Figure 11: Mean ADC pulse height measured with the tube ZH5126 as a function of the applied high voltage value (open circles) in magnetic fields of 1.44 T (open circles) and 0 T (filled circles).